

Vortex microavalanches in superconducting Pb thin films

H.A. Radovan and R.J. Zieve

Physics Department, University of California at Davis, Davis, CA 95616

Local magnetization measurements on 100 nm type-II superconducting Pb thin films show that flux penetration changes qualitatively with temperature. Small flux jumps at the lowest temperatures gradually increase in size, then disappear near $T = 0.7T_c$. Comparison with other experiments suggests that the avalanches correspond to dendritic flux protrusions. Reproducibility of the first flux jumps in a decreasing magnetic field indicates a role for defect structure in determining avalanches. We also find a temperature-independent final magnetization after flux jumps, analogous to the angle of repose of a sandpile.

I. INTRODUCTION

Magnetic fields penetrate type-II superconductors in the form of vortices. Pinning sites inside the sample maintain a spatial variation in the vortex density, with an accompanying current density j . The resulting Lorentz force drives further flux penetration. In the Bean critical-state model, vortex motion is triggered whenever the current density exceeds a critical current density j_c , thereby maintaining a current density j_c everywhere in the material [1]. The constant current density corresponds to a constant vortex density gradient, much like the surface of a sandpile with grains poised to flow. As the applied field changes, the flux density adjusts steadily, giving rise to a smooth hysteresis loop $B(H)$ [2].

However, in many situations abrupt flux jumps appear, corresponding to near-instantaneous motion of many vortices. While individual moving vortices are like single grains falling down the side of a sandpile, flux jumps resemble an avalanche of many grains. In 1968 Heiden et al. measured jumps 10 to 10,000 vortices in size in tubular Pb-In alloys [3]. Since then magnetic instabilities have been observed down to $0.001 T_c$ in YBaCuO [4, 5] and up to $0.95T_c$ in Nb [6]. Other superconductors showing flux jumps include Nb-Ti [7], Pb-In [8], and MgB₂ [9].

The most common explanation for the flux jumps is a magnetothermal instability. Moving flux increases the local temperature. The temperature change reduces j_c , which triggers further vortex motion. This feedback produces the vortex avalanche. If the sample recovers without quenching completely, there are small steps in the magnetic hysteresis loop rather than full jumps to zero magnetization. Other proposed sources for the avalanches include self-organized criticality [10], dynamical instabilities [5], and stick-slip dynamics [11].

Several contrasting temperature and field dependences have been observed. Most commonly flux instabilities occur at low magnetic fields, where the critical current density is largest, but some of the YBaCuO work finds flux jumps only at *large* fields [4, 5]. Jumps range in size from a few vortices, requiring careful time and voltage resolution to identify that a jump occurred, to “complete” avalanches that occur throughout the sample and reduce the sample magnetization to zero. Generally when a sample displays complete or near-complete flux jumps the avalanche size distribution has a sharp peak, while in other cases the distribution is broad, with either power-law or exponential behavior. A few recent studies have found *both* behaviors, fairly small jumps with a broad size range and

larger avalanches with a single characteristic size, at different temperatures in a single sample. In Nb samples complete flux jumps occur at the lowest investigated temperatures and smaller avalanches at higher temperatures [6, 12, 13], with a sharp change in jump size. On the other hand, in MgB₂ flux jumps gradually get larger as temperature increases without ever becoming complete [9, 14].

Here we report local Hall probe measurements in a new system, type-II Pb thin films. We find flux avalanches for temperatures below $0.7T_c$, with both large and small jumps at different temperatures. The behavior is most similar to that of MgB₂, with larger jumps observed only at relatively high temperature. We investigate sample, field history, magnet ramp rate, and maximum cycling field dependence. The properties independent of external parameters are the field of occurrence and size of the first microavalanche, and the final magnetization after a jump. We argue that an interplay between the vortex density and the microstructure is at the origin of the flux instabilities. We find that the changes in jump size with temperature arise from the earlier triggering of avalanches at low temperature combined with the near-constant final magnetization.

II. EXPERIMENTAL

We fabricate 100 nm Pb films on 4 mm by 4 mm Si substrates by resistive evaporation at 2 \AA/s at room temperature. A 40 nm Ge capping layer prevents Pb oxidation. The thickness is calibrated with a profilometer. We prepared the two samples discussed in this paper under nominally identical conditions. The upper critical field was measured in a Quantum Design MPMS XL SQUID system. For $T = 0 \text{ K}$, B_{c2} extrapolates to 1319 G. We estimate the Ginzburg-Landau parameter at $\kappa = 1.23$, comfortably within the type-II regime.

For magnetization measurements we use a semiconductor Hall probe [15] with an active area of $400 \mu\text{m}^2$ and a sensitivity of $900 \text{ m}\Omega/\text{kG}$. Applied magnetic fields reach 400 Oe. Most of the measurements at $T > 4.2 \text{ K}$ were carried out in a simple He-dewar insert with temperature stability better than $\pm 1 \text{ mK}$. For Sample B we extended the data down to 0.27 K on a pumped ³He cryostat with stability better than $\pm 10 \text{ mK}$. The critical temperature for all samples is the bulk value, $T_c = 7.2 \text{ K}$. For comparison to bulk type-I Pb we used a disk with a diameter of 4 mm and a thickness of $400 \mu\text{m}$.

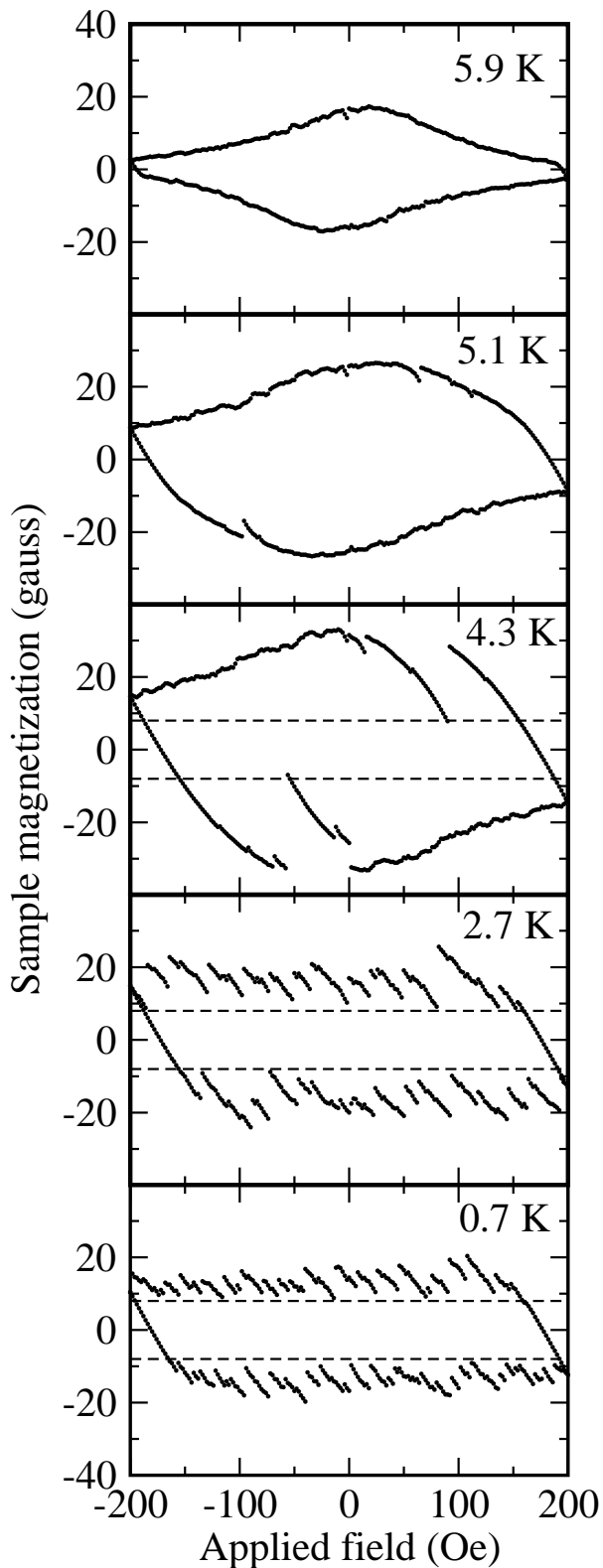


FIG. 1: Magnetic hysteresis loops at several temperatures for Sample B. All graphs have the same vertical scale. The dashed horizontal lines at ± 8 gauss in each of the bottom three graphs illustrate the temperature-independence of the magnetization just after an avalanche.

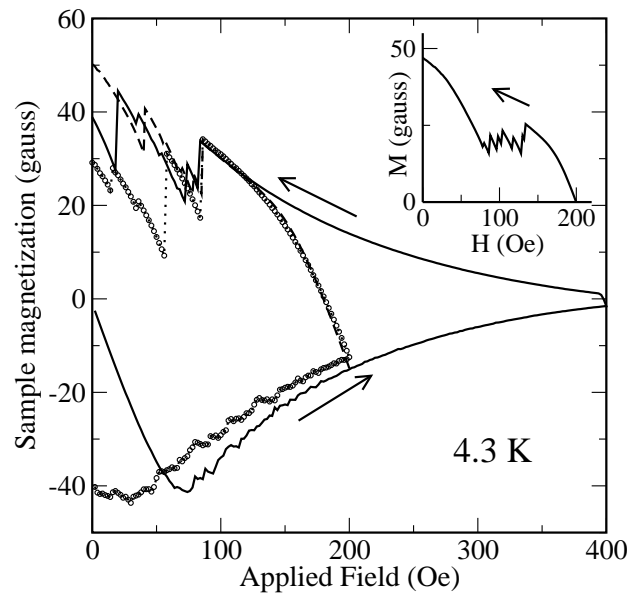


FIG. 2: Hysteresis loops for Sample B with maximum field 200 Oe (circles and dashed line), and 400 Oe (solid line). Note the lack of jumps at higher fields, and the reproducibility of the field for the first jump. Inset: descending branch of hysteresis loop for Sample A at 4.57 K.

III. RESULTS AND DISCUSSION

Figure 1 shows the flux jump characteristics for our Sample B. The maximum field of 200 Oe allows full flux penetration at all temperatures. The horizontal axis shows the applied, external field, with no adjustment for demagnetization effects. The step size is 2 Oe, with 2 seconds between steps. The width and qualitative flux jump behavior in the hysteresis loops are fully reproducible on different cooldowns. Just below T_c the hysteresis loops are smooth on the scale of our measurements, as represented in Figure 1 by the 5.9 K hysteresis loop. We do not have the temporal resolution of Behnia et al., who show that tiny flux jumps may drive even magnetization changes that appear smooth [13]. Cooling produces first a few small avalanches (5.1 K), then larger, often nearly complete jumps which coexist with the small ones (4.3 K). Both large and small jumps occur preferentially on the decreasing branch of the hysteresis loop, appearing on the increasing branch only at lower temperatures. On further cooling, the small jumps remain, while the large ones gradually shrink until the two types are no longer clearly distinguishable. The hysteresis loops also narrow and flatten as temperature decreases, with the *final* magnetization just after a flux jump nearly temperature-independent.

The flux jumps occur only at sufficiently small fields. The solid hysteresis loop of Figure 2 has maximum field 400 Oe, while the dashed curve (descending branch only) begins at 200 Oe. The third curve, represented by circles and a dotted line, was taken seven weeks later after thermally cycling to room temperature. It also has maximum field 200 Oe. The

hysteresis loops display some noise on the increasing branch but no clear avalanches. Noise on the increasing branch also develops through the top three frames of Figure 1. The noisy region, which is confined to low applied fields and increases in range as temperature decreases, may be a precursor for the avalanches on the increasing branch at lower temperatures. On the decreasing branch of the hysteresis loop, all three curves of Figure 2 have their first flux jump at the same field, regardless of the field history. This onset field does depend on temperature, increasing as temperature decreases. By 300 mK, the onset field for jumps exceeds 300 gauss.

Sample A, which we measured only above 4.2 K, shows generally similar behavior. One difference is that at one temperature (4.57 K), there is a minimum applied field for avalanches as well as a maximum field. The inset of Figure 2 illustrates this behavior after the sample is cooled through T_c in an applied field of 200 gauss; the same effect occurs upon cooling in zero field. Having flux jumps confined to such a limited field range requires a particularly delicate balance between stable and unstable regimes. The different behavior of our two samples also highlights the importance of the precise defect structure in the flux jump patterns.

Among previously measured materials, MgB_2 behaves most like our Pb samples. MgB_2 shows flux jumps below about $t = T/T_c = 0.25$, with the jumps steadily shrinking as t decreases; and smooth changes in magnetization from $t = 0.25$ to $T_c = 39\text{K}$ [9, 14]. As in our samples, the MgB_2 instabilities at the highest temperatures occur primarily for decreasing magnetic field, perhaps because of an additional heat load from annihilation of vortices with antivortices [16].

On a microscopic level, both magneto-optical (MO) imaging and Bitter patterns in a variety of materials show that many flux jumps come from sudden dendritic protrusions of high-vortex-density regions into the specimen [6, 14, 16, 17, 18, 19]. In MgB_2 , MO shows quasi-one-dimensional dendritic fingers at the lowest temperatures, and branched structures at higher temperatures, with a similar behavior found in computational work [14, 20]. Although MO and magnetization measurements have rarely been carried out on the same sample, the slight increase in avalanche size with temperature in MgB_2 apparently corresponds to the increased branching of the dendrites, which allows more flux motion [14]. In Nb, however, MO shows dendritic “fingers” at both low [3] and intermediate [6] temperatures, while magnetization measurements consistently find the largest avalanches at low temperatures. We suggest that the complete flux jumps found in Nb at the lowest temperatures differ fundamentally from the partial jumps in MgB_2 . Indeed, at low temperatures the flux front in Nb moves in spurts but without branching [6]. With no optical data on Pb, we cannot firmly identify our flux jumps as coming from fingering events, but similarities between the jumps in our samples and in MgB_2 make this a good possibility. The biggest difference is the quantitative observation that our high-temperature avalanches, while not complete, are substantially larger than those in MgB_2 .

We have eliminated various possible artifacts as the source of our results. First, with no sample or with a bulk Pb disk, the Hall probe yields no fluctuations in the signal down to

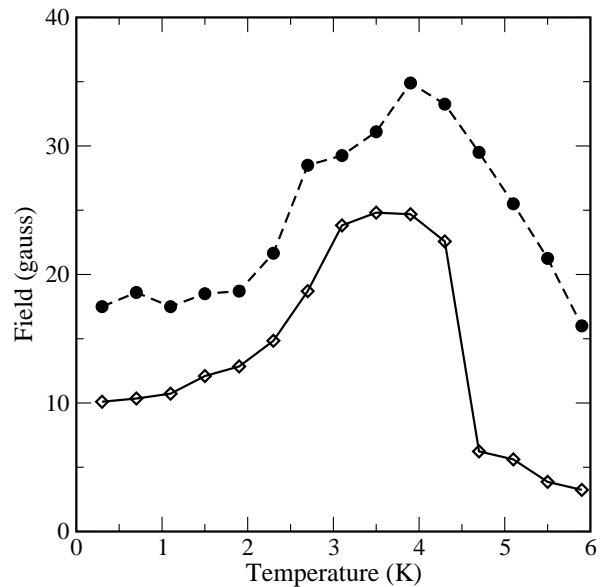


FIG. 3: Half the maximum width of hysteresis loop (filled circles) and size of second-largest avalanche (diamonds). The two curves track each other below 3 K.

the lowest temperatures. Hall probe excitation currents from $5\ \mu\text{A}$ to 1 mA at $T = 0.3\ \text{K}$ do not change the loop width or jump sizes, so heat from the Hall current is not a factor within this range. Increasing the excitation current to 5 mA, however, does reduce the width notably. The avalanches are also independent of ramp rates from 0.2 Oe/s to 3.3 Oe/s, data point spacings from 1 Oe to 10 Oe, and history effects such as the maximum field achieved during a hysteresis loop or cooling in zero or non-zero field.

Figure 3 displays the maximum magnetization as a function of temperature for Sample B. The values used are half the maximum difference between the ascending and descending branches of a hysteresis loop. In critical-state models, the hysteresis loop width is directly proportional to the critical current density j_c of the material and increases steadily as temperature drops. We find this behavior above 3.9 K, but on further decreasing temperature the magnetization drops rapidly. The decrease becomes less steep but persists down to our lowest temperature of 0.27 K, where the width is 60% below its maximum value. This narrowing of the hysteresis loop is also visible in Figure 1. Once the flux jumps begin, the idea of a critical state may no longer apply. The numerous low temperature avalanches significantly depress the current carrying ability of type-II Pb films. Although vortex avalanches are often attributed to thermomagnetic instabilities, the reduction of the loop width shows that achieving a global critical current is not a requirement for triggering a jump. Qualitatively similar behavior was recently found in MgB_2 films, where j_c drops up to 40% below $t = 0.25$ [9, 14].

Along with the maximum magnetization, we plot the size of the second-largest avalanche at each temperature. We choose the second-largest rather than the largest avalanche because there is less variation in size, although using the largest

avalanche gives similar results. The jump size at low temperature decreases roughly as T^3 , approaching a finite value as $T \rightarrow 0$. Significantly, the loop width and avalanche size track each other closely, indicating that the final magnetization is nearly independent of temperature. Again, this point is illustrated directly in Figure 1, where the dashed lines at ± 8 gauss for the bottom three frames show how near to this field the avalanches end. The final magnetization does vary between cooldowns, and was about 12 gauss and 19 gauss for two other cooldowns on Sample B. The variation may stem from the heat-sinking of the substrate or from changes in the location of the Hall probe.

Our measurements show that the flux jump trigger changes with temperature. At the higher temperatures, the data are consistent with thermomagnetic instabilities within a Bean-type critical state model, since jumps begin only when the magnetization lies along the ideal hysteresis loop. At lower temperatures, the narrowing hysteresis loops show that the avalanches begin before the sample reaches a global critical state. The nearly constant envelope of the magnetization with applied field shows that at low temperatures the flux jump trigger becomes independent of field. The narrowing of the hysteresis loop begins at about the same temperature where flux jumps start to occur for increasing field. If the jumps correspond to dendrites of flux entering the sample, the dendrites themselves could produce local field variations that trigger further avalanches while the sample is well away from a global critical state.

Furthermore, the uniform final magnetization shows that the cessation of the avalanches has a different mechanism from their onset, and is independent of whether the initial trigger is global or local. The temperature-independence of the final magnetization suggests that the jumps do not halt simply from a thermal recovery. Since the lowest temperature flux jumps are also the smallest, the system should not reach as high a temperature, leaving no clear origin for the constant final magnetization. Rather, the moving vortex system seems to recover upon reaching a particular current density which acts much like the angle of repose of a sandpile. Once again our sample behaves much like MgB_2 , where recent measurements find that the local field just after an avalanche has a reproducible maximum value of about 120 gauss [21].

As noted above, the three loops of Figure 2 have their first flux jumps at nearly identical fields. In fact both the size and the applied field of the first avalanche are robust against changes in ramp rate, maximum cycling field, and field history, although they are sample dependent. However, the sharp peaks in size disappear quickly. Figure 4 shows histograms for the first three avalanches. The data for each sample come from a series of 20 identical half-loops with ramp rate 1 Oe/s on the decreasing branch. The field and avalanche size for the first jump is $H = (130 \pm 1)$ Oe with $\Delta B = 2 - 3$ G for Sample A and $H = (84 \pm 3)$ Oe with $\Delta B = 10 - 15$ G for Sample B. The parameters are particularly repeatable for Sample A, but even the distribution in Sample B is narrower than that of later avalanches. The second avalanche is broader than the first but still has a characteristic size. The third and subsequent avalanches follow a broader distribution weighted

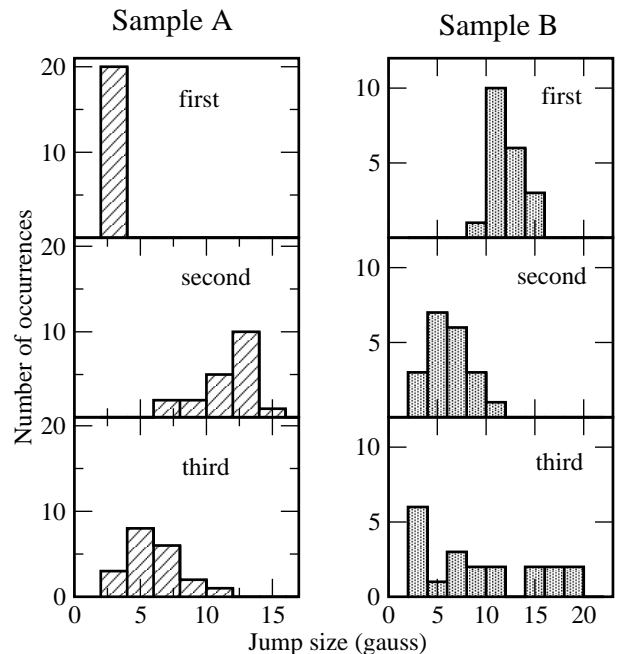


FIG. 4: Size distributions for first three avalanches for Sample A at 4.35 K and Sample B at 4.6 K.

towards small sizes. As temperature decreases, the distinction between the early and later avalanches goes away, disappearing entirely by 2.7 K. The reproducibility of the field for the first avalanche vanishes likewise. A possible interpretation is that the initial flux jumps from a smooth flux front are primarily influenced by defects in the sample. The similarities of the first few jumps on different hysteresis loops reflect the nearly identical flux penetration. Small irreproducibilities in the first few jumps leave unique flux profiles. These magnetization patterns, as well as the defect structure, influence later flux jumps, destroying further quantitative likeness among hysteresis loops. The characteristic initial jump size disappears at low temperature because once flux jumps occur for increasing field, even the initial magnetization pattern on the decreasing branch varies among loops.

For both our samples the individual avalanches range in size from about 1 G to 16 G, corresponding to a change of 20 to 300 vortices under the Hall probe. The similar size range indicates that the same general mechanism is responsible for these flux front instabilities. Figure 5 shows the size distribution of flux jumps for Sample B during 20 cycles at $T = 4.3$ K, where flux jumps occur only for decreasing field, and three loops at $T = 300$ mK with flux jumps on both branches. We omit the first two flux jumps at 4.3 K because of their atypical size distribution, as discussed above. Interestingly, at 4.3 K the avalanche sizes do *not* actually have a sharp division between large and small; it appears so for an individual hysteresis loop only because there are so few large jumps. Both exponential [3, 18] and power-law [6, 12] distributions are reported in the literature. For our data a power law form works much better than an exponential for the 300 mK data, and somewhat bet-

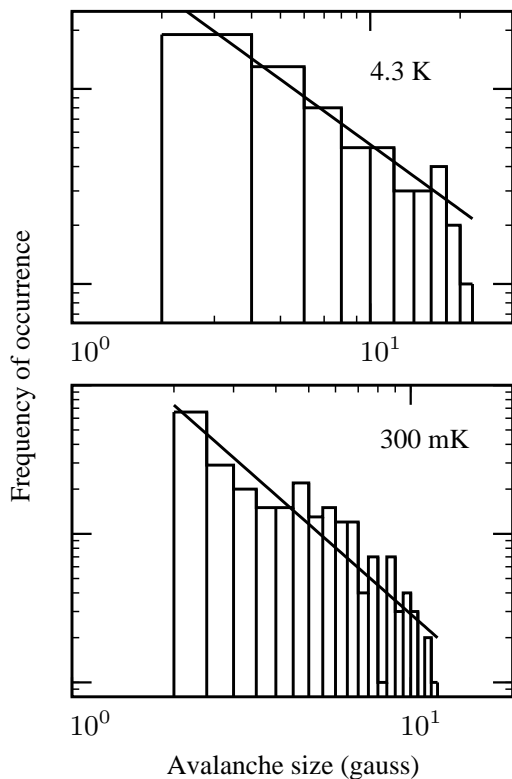


FIG. 5: Size distributions for Sample B at 4.3 K (top) and 300 mK (bottom), on log-log scales. The first two avalanches per loop are omitted from the 4.3 K data. Solid lines are power law fits, with exponents -1.09 for 4.3 K and -2.01 for 300 mK.

ter at 4.3 K. The best-fit powers for these two temperatures are very close to -2 and -1 , respectively. The special character of the first two avalanches may account for some of the controversy over whether the size distribution follows power law or exponential behavior. Including them at 4.3 K changes the best fit from power law to exponential, although neither function fits the distribution especially well.

Finally, since the repeatability of our initial avalanches suggests that defect patterns influence the flux jumps, we comment on microstructure. Our Pb thin films experience significant extrinsic stress from their adhesion to the Si substrate. The thermal expansion coefficients of Si and Pb differ by one order of magnitude. Upon thermal cycling Pb releases com-

pressive stress by atomic diffusion, which forms hillocks and voids. Another source of stress is the 8.9% lattice misfit between film and substrate, and the 12.4% misfit between the Pb film and the Ge capping layer. The film releases this stress through formation of predominantly edge-type dislocations [22]. Any two samples have different defect structures, and the existence of a minimum field for avalanches in only one of our samples shows that details of the defects can strongly affect flux stability. We have also tested a bulk Pb disk, which is high purity and has no misfit stress. The disk does not support flux instabilities in any temperature or field range, during flux entry or exit. Although bulk lead is a type-I superconductor, MO investigations show that field penetration begins with flux tubes containing 500 to 1000 flux quanta [23]. The flux tubes form a hexagonal lattice much like the Abrikosov vortex lattice, and in principle should be able to undergo avalanching similar to that of quantized vortices in type-II materials. The absence of microavalanches in the bulk material is consistent with its relative scarcity of defects.

IV. SUMMARY

We report local magnetic measurements on 100 nm Pb type-II thin films for temperatures down to 0.27 K. The hysteresis loops display several flux penetration patterns as a function of temperature, starting out with many microavalanches at the lowest temperature, then fewer and bigger ones until the classical critical-state type flux penetration is reached for $T/T_c > 0.7$. We draw attention to two surprisingly robust features: the size and location of the first instability in a decreasing magnetic field, and the final magnetization after an avalanche. The occurrence of the first instability varies little with external parameters, but is sample dependent. The final magnetization also varies among cooldowns, but is nearly temperature-independent for a given cooldown from room temperature. Finally, we note that the similarity of our work and recent measurements on MgB_2 films shows that the underlying mechanisms governing vortex motion are not specific to MgB_2 .

V. ACKNOWLEDGEMENT

We thank P. Klavins for technical assistance. This work was supported by the NSF under DMR-9733898.

-
- [1] C.P. Bean, "Magnetization of high-field superconductors," *Rev. Mod. Phys.* **36**, 31 (1964).
 - [2] A.M Campbell and J.E. Evetts, "Flux vortices and transport currents in type II superconductors," *Adv. Phys.* **21**, 199 (1972).
 - [3] C. Heiden and G.I. Rochlin, "Flux jump size distribution in low- κ type-II superconductors," *Phys. Rev. Lett.* **21**, 691 (1968).
 - [4] G.T. Seidler, C.S. Carrillo, T.F. Rosenbaum, U. Welp, G.W.

- Crabtree, and V.M. Vinokur, "Vanishing magnetization relaxation in the high field quantum limit in $\text{YBa}_2\text{Cu}_3\text{O}_{7-\delta}$," *Phys. Rev. Lett.* **70**, 2814 (1993).
- [5] R.J. Zieve, T.F. Rosenbaum, H.M. Jaeger, G.T. Seidler, G.W. Crabtree, and U. Welp, "Vortex avalanches at one thousandth the superconducting transition temperature," *Phys. Rev.* **B53**, 11849 (1996).

- [6] S.S. James, S.B. Field, J. Seigel, and H. Shtrikman, "Scanning Hall probe microscope images of field penetration into niobium films," *Physica* **C332**, 445 (2000).
- [7] S. Field, J. Witt, F. Nori, and X.S. Ling, "Superconducting vortex avalanches," *Phys. Rev. Lett.* **74**, 1206 (1995).
- [8] S.T. Stoddart, H.I. Mutlu, A.K. Geim, and S.J. Bending, "Microscopic investigation of the flux dynamics of type-II superconducting films," *Phys. Rev.* **B47**, 5146 (1993).
- [9] Z.W. Zhao, S.L. Li, Y.M. Ni, H.P. Yang, Z.Y. Liu, H.H. Wen, W.N. Kang, H.J. Kim, E.M. Choi, and S.I. Lee, "Suppression of superconducting critical current density by small flux jumps in MgB₂ thin films," *Phys. Rev.* **B65**, 064512 (2002).
- [10] R.A. Richardson, O. Pla, and F. Nori, "Confirmation of the modified Bean model from simulations of superconducting vortices," *Phys. Rev. Lett.* **72**, 1268 (1994).
- [11] W. Barford, "Avalanches in the Bean critical-state model," *Phys. Rev.* **B56**, 425 (1997).
- [12] E.R. Nowak, O.W. Taylor, L. Liu, H.M. Jaeger, and T.I. Selinder, "Magnetic flux instabilities in superconducting niobium rings—tuning the avalanche behavior," *Phys. Rev.* **B55**, 11702 (1997).
- [13] K. Behnia, C. Capan, D. Maily, and B. Etienne, "Internal avalanches in a pile of superconducting vortices," *Phys. Rev.* **B61**, 3815 (2000).
- [14] T.H. Johansen, M. Baziljevich, D.V. Shantsev, P.E. Goa, Y.M. Galperin, W.N. Kang, H.J. Kim, E.M. Choi, M.S. Kim, and S.I. Lee, "Dendritic magnetic instability in superconducting MgB₂ films," *Europhys. Lett.* **59**, 599 (2002) [arXiv:cond-mat/0104113].
- [15] AREPOC Ltd., Slovakia.
- [16] T.H. Johansen, M. Baziljevich, D.V. Shantsev, P.E. Goa, Y.M. Galperin, W.N. Kang, H.J. Kim, E.M. Choi, M.S. Kim, and S.I. Lee, "Dendritic flux patterns in MgB₂ films," *Supercond. Sci. Technol.* **14**, 726 (2001).
- [17] B.U. Runge, U. Bolz, J. Boneberg, V. Bujok, P. Brull, J. Eisenmenger, J. Schiessling, and P. Leiderer, "Magneto-optic characterization of defects and study of flux avalanches in high- T_c superconductors down to nanosecond time resolution," *Laser Phys.* **10**, 53 (2000).
- [18] C.A. Duran, P.L. Gammel, R.E. Miller, and D.J. Bishop, "Observation of magnetic-field penetration via dendritic growth in superconducting niobium films," *Phys. Rev.* **B52**, 75 (1995).
- [19] P. Leiderer, J. Boneberg, P. Brull, V. Bujok, and S. Herminghaus, "Nucleation and growth of a flux instability in superconducting YBa₂Cu₃O_{7-x} films," *Phys. Rev. Lett.* **71**, 2646 (1993).
- [20] I. Aranson, A. Gurevich, and V. Vinokur, "Vortex avalanches and magnetic flux fragmentation in superconductors," *Phys. Rev. Lett.* **87**, 067003 (2001).
- [21] F.L. Barkov, D.V. Shantsev, T.H. Johansen, P.E. Goa, W.N. Kang, H.J. Kim, E.M. Choi, and S.I. Lee, "Local threshold field for dendritic instability in superconducting MgB₂ films," *Phys. Rev.* **B67**, 064513 (2003).
- [22] K.-N. Tu, J.W. Mayer, and L.C. Feldman, *Electronic thin film science: for electrical engineers and materials scientists*, p. 168 (Macmillan, New York, 1992).
- [23] H. Kirchner, "Ein hochauflösendes magnetooptisches Verfahren zur Untersuchung der Kinematik magnetischer Strukturen in Supraleitern," *Phys. Stat. Sol.* **A4**, 531 (1971).